Journal of Materials Chemistry C

PAPER

View Article Online
View Journal | View Issue

Cite this: J. Mater. Chem. C, 2015, 3, 6549

Ionic liquid–water mixtures and ion gels as electrolytes for organic electrochemical transistors†

Zhihui Yi,[a] Giovanniantonio Natale,[a] Prajwal Kumar,[a] Eduardo Di Mauro,[b] Marie-Claude Heuzey,[a] Francesca Soavi,[c] Iryna I. Perepichka,[d] Sunil K. Varshney,[d] Clara Santato*[b] and Fabio Cicoira*[a]

Received 13th March 2015,
Accepted 2nd June 2015

DOI: 10.1039/c5tc00712g

www.rsc.org/MaterialsC

Organic Electrochemical Transistors (OECTs) are widely investigated for applications in bioelectronics. Ionic liquids (ILs) are, in principle, interesting candidates as gating media in OECTs. Nevertheless, ILs can exhibit excessively high viscosity that prevents their straightforward application in OECTs. Here we report two processing approaches to apply the highly viscous ionic liquid triisobutyl(methyl)phosphonium tosylate (Cyphos® IL 106) in OECTs based on poly(3,4-ethylenedioxythiophene) polystyrenesulfonate (PEDOT:PSS), namely IL–H_2O binary mixtures and ion gels. The use of Cyphos® IL 106–H_2O binary mixtures and ion gels as gating media determines an increase of the OECT modulation, with respect to the pure ionic liquid. This increase cannot be explained simply by the change of the viscosity and ionic conductivity of the ionic liquid–H_2O mixtures with the increase of the H_2O content. Using high surface area activated carbon gates, ON/OFF ratios as high as 5000 are achieved with Cyphos® IL 106–H_2O mixtures at 5 and 10% H_2O v/v.

Introduction

Ionic liquids are molten salts at relatively low temperature (typically below 100 °C) that possess chemical and electrochemical stability, optical transparency, and low volatility.[1–4] Owing to these unique properties, ionic liquids have found several technological applications, such as solvents for organic and inorganic synthesis and (bio)catalysis, electrolytes in electrochemical devices, and media for enzyme storage and reactions.[2,3,5–10] In particular, phosphonium ionic liquids are interesting for their thermal stability and wide electrochemical stability window.[11]

The diverse molecular structures of the anionic and cationic species constituting an ionic liquid can give rise to a variety of interactions, such as electrostatic, van der Waals, and hydrogen bonding. These interactions control the physicochemical properties of ionic liquids, such as ionic conductivity and viscosity.[1–4,12] The physicochemical properties of ionic liquids can be tailored for specific applications by mixing with a solvent.[13]

Electrolyte-gated organic transistors make use of organic materials for the transistor channel and of electrolytes as the gating media. These transistors exhibit current modulations of several orders of magnitude upon application of gate voltages as low as 0.5–2 V.[14–19] On the basis of their operating mechanism, electrolyte-gated transistors can be divided into two groups: electrical double layer transistors and electrochemical transistors. In electrical double layer transistors, current modulation relies on electrostatic doping of the channel at the channel/electrolyte interface. In electrochemical transistors, the current is modulated by doping/dedoping of the bulk of the organic channel by electrolyte ions. Organic Electrochemical Transistors (OECTs) are investigated in bioelectronics because of their low operating voltage, which is compatible with aqueous media, where biological processes take place.[20–23] Depending on the targeted application, OECTs can make use of various types of electrolytes, including aqueous or organic solutions, ionic liquids and gels. Among the properties that make electrolytes suitable for OECTs are wide electrochemical stability window, good ionic conductivity and low viscosity.

Here we investigate the use of a highly viscous ionic liquid, *i.e.* triisobutyl(methyl)phosphonium tosylate (Cyphos® IL 106, inset Fig. 1a), as electrolyte for OECTs. Cyphos® IL 106 is interesting

[a] Department of Chemical Engineering, Polytechnique Montréal, CP 6079, Succursale Centre-Ville, Montréal, Québec H3C 3A7, Canada. E-mail: fabio.cicoira@polymtl.ca
[b] Department of Engineering Physics, Polytechnique Montréal, CP 6079, Succursale Centre-Ville, Montréal, Québec H3C 3A7, Canada. E-mail: Clara.santato@polymtl.ca
[c] Department of Chemistry "Giacomo Ciamician", Università di Bologna, Via Selmi, 2, 40126, Italy
[d] Polymer Source, Inc., 124 Avro street, Dorval, Quebec H9P 2X8, Canada

† Electronic supplementary information (ESI) available: Device structures; OECT current modulation as a function of V_g for pure ionic liquid and mixtures at 5%, 50%, 90%, 95%, 99% H_2O v/v; transfer curves of OECTs with PEDOT:PSS gate electrodes; comparison of transfer curves obtained with NaCl and Cyphos® IL 106/H_2O mixtures; Table ESI1 (ionic conductivities) and Table ESI2 (ON/OFF ratios). See DOI: 10.1039/c5tc00712g

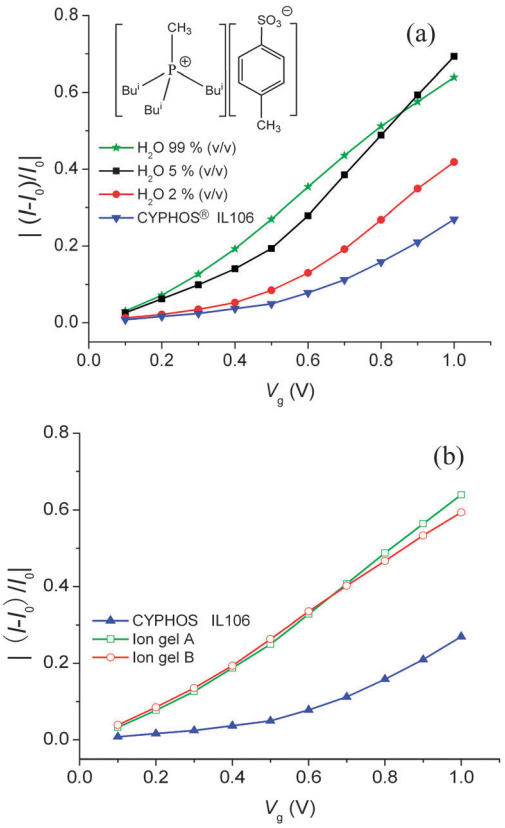

Fig. 1 Current modulation $|(I - I_0)/I_0|$ *vs.* V_g for PEDOT:PSS OECTs making use of a PEDOT:PSS gate for: (a) Cyphos® IL 106, and Cyphos® IL 106–H_2O mixtures at 2%, 5%, 99% H_2O v/v and (b) pure Cyphos® IL 106 and ion gels A (SMMAS : Cyphos® IL 106 1 : 10 w/w) and B (SMMAS : Cyphos® IL 106 1 : 5 w/w). $V_d = -0.2$ V. Inset (a): molecular structure of Cyphos® IL 106. The current modulation is obtained from transient measurements (current *vs.* time at different V_g) and it is defined as $|(I - I_0)/I_0|$, where I is the drain–source current at $V_g \neq 0$ V and the I_0 is the current at $V_g = 0$ V taken before each V_g pulse. Lines are guides to the eye.

for bioelectronic applications because of its miscibility with aqueous media, electrochemical stability and ability to act as a reservoir for enzymes and mediators in electrochemical sensors.[9,11] Furthermore, it is an active and selective solvent for conversion of fructose into hydroxymethylfurfural without any catalyst addition.[24,25] The interaction between Cyphos® IL 106–H_2O binary mixtures and thin films of the conducting polymer poly(3,4-ethylenedioxythiophene) doped with tosylate has been recently explored.[26]

Specifically, we propose two processing approaches to employ Cyphos® IL 106 as electrolyte for OECTs. The first approach consists in using ionic liquid–H_2O binary mixtures, while the second consists in incorporating the ionic liquid into an ion gel. To explore the possibility to establish a correlation between the physicochemical properties of the gating media and device characteristics, we studied the viscosity and the ionic conductivity of the electrolytes.

Results and discussion

The gating properties of Cyphos® IL 106–H_2O binary mixtures were first investigated on planar OECTs employing the conducting polymer poly(3,4-ethylenedioxythiophene) doped with polystyrene sulfonate (PEDOT:PSS) as the transistor channel and the gate electrode (Fig. ESI1 in ESI†). The OECT current modulation, $|(I - I_0)/I_0|$, where I and I_0 are the drain–source currents at $V_g \neq 0$ V and at $V_g = 0$ V, is shown as a function of the gate–source voltage, V_g, for pure Cyphos® IL 106 and for Cyphos® IL 106–H_2O binary mixtures (Fig. 1a). Mixing Cyphos® IL 106 with 2% H_2O v/v (*i.e.* 98% Cyphos® IL 106 v/v) leads to a considerable increase of the current modulation with respect to pure Cyphos® IL 106 (*e.g.* from ~0.15 to ~0.25 at $V_g = 0.8$ V). Increasing the H_2O content to 5% v/v further increases the modulation up to ~0.5. Upon further H_2O addition, *i.e.* for 50%, 90%, 95%, and 99% H_2O v/v, the OECT modulation remains substantially unchanged (Fig. 1a and Fig. ESI2 (ESI†)). The transfer curves of OECTs using as the gating medium pure Cyphos® IL 106 and Cyphos® IL 106–H_2O mixtures (Fig. ESI3 (ESI†)) show that the drain–source current (I_d) decreases with the increase of V_g, consistently with the depletion mode of operation of PEDOT:PSS OECTs.

To gain insight into the improvement of the OECT performance upon H_2O addition to Cyphos® IL 106, we investigated the effect of H_2O on viscosity and ionic conductivity. As shown in Fig. 2a, the Newtonian viscosity (η) decreases dramatically from about 4000 mPa s, for the pure Cyphos® IL 106, to about 110 mPa s, for a mixture containing 10% H_2O v/v. For higher H_2O content, the viscosity decreases gradually to a few mPa s (*e.g.* about 3 mPa s for 70% H_2O v/v). The presence of complex interactions between H_2O and Cyphos® IL 106 is revealed by Fig. 2a, which shows that the viscosity of the mixtures always lies below the line corresponding to the viscosity of an ideal mixture (the dashed line between the values of the viscosities of the two pure components). The effect of H_2O on the viscosity can be further understood considering the results reported in the inset of Fig. 2a, where the dynamic storage modulus, G', and loss modulus, G'', are shown for the pure Cyphos® IL 106 and for Cyphos® IL 106–H_2O mixture with 5% H_2O v/v. The addition of H_2O causes a decrease in the values of both G' and G''. The lower values of G' and G'' are compatible with a scenario where the interactions between ions with opposite polarity are partially reduced, thus leading to higher ion mobility. G' of the pure Cyphos® IL 106 shows a strong deviation from the classic Maxwell behaviour of fluids at low frequencies, while the viscosity is completely Newtonian.[27]

The ionic conductivity, as measured by a conductivity meter, increases from a few fractions of mS cm^{-1} for pure IL up to 12 at 70% H_2O v/v, then decreases to 8 mS cm^{-1} at 90%, and 1.5 mS cm^{-1} at 99% H_2O v/v (Table ESI1 (ESI†)). Upon addition of molecular solvents to viscous ionic liquids, a significant drop of the viscosity and an increase of the ionic conductivity, followed by a decrease with further addition of solvent, are generally expected.[28–32]

Ion gels have recently found application in bioelectronics, *e.g.* for sub cutaneous recordings[33] and DNA sensing.[34] We prepared ion gels from Cyphos® IL 106 and the triblock copolymer polystyrene-*b*-poly(methylmethacrylate)-*b*-polystyrene (SMMAS, PolymerSource Inc.) at SMMAS : Cyphos® IL 106 mass ratios 1 : 10 (ion gel A) and 1 : 5 (ion gel B). The OECT modulations obtained with ion gels A

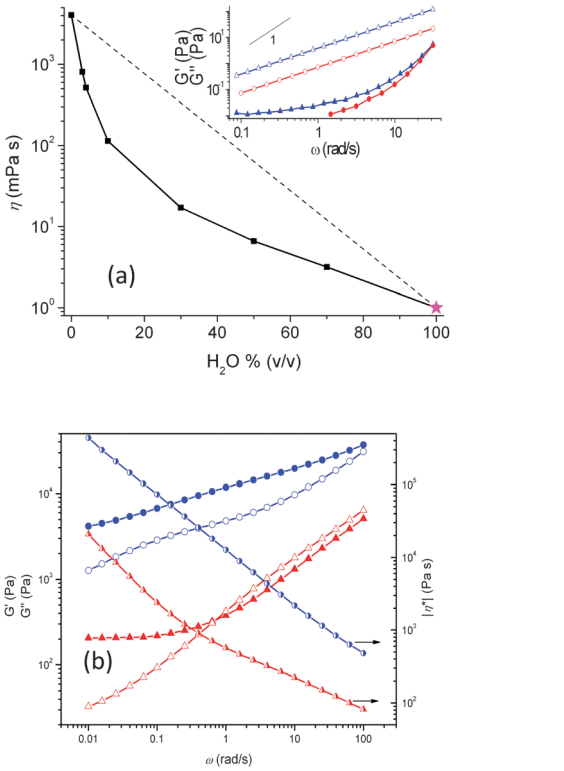

Fig. 2 (a) Shear viscosity (η) of pure Cyphos® IL 106, Cyphos® IL 106–H_2O mixtures (2%, 5%, 10%, 30%, 50%, 70% H_2O v/v, filled black squares) and viscosity of pure H_2O (filled star symbol). The dashed line between the values of the viscosities of the two pure components represents the viscosity of an ideal mixture. Inset: variation of the storage (G', solid symbols) and loss (G'', empty symbols) modulus with the angular frequency for pure Cyphos® IL 106 (blue triangles) and Cyphos® IL 106–H_2O mixture at 5% H_2O v/v (red circles). The slope 1 is reported as a reference for the classic behavior of G' for a liquid, at low frequency. (b) Storage modulus (G', solid symbol), loss modulus (G'', empty symbol) and complex viscosity η^* (half-filled symbol) of ion gel A (triangle) and ion gel B (circle).

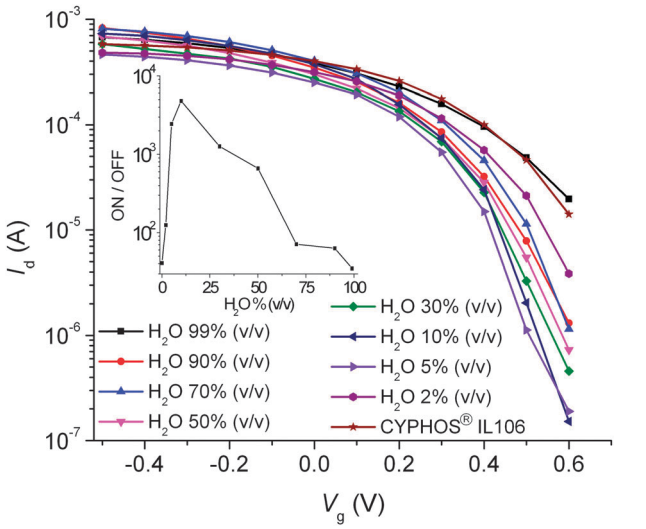

Fig. 3 Transfer characteristics of PEDOT:PSS OECTs making use of activated carbon as the gate electrode and different Cyphos® IL106–H_2O mixtures as the gating media. V_d = −0.5 V. Inset: ON/OFF ratio for different Cyphos® IL 106–H_2O mixtures.

and B (corresponding transfer curves shown in Fig. ESI4 (ESI†)) are similar and both higher than those observed with analogue OECTs making use of pure Cyphos® IL 106 (Fig. 1b). At V_g = 0.8 V, the modulation is ~0.5 for both ion gels and ~0.15 for pure Cyphos® IL 106. The ionic conductivity measured by electrochemical impedance spectroscopy for ion gel A is 3×10^{-2} mS cm^{-1} whereas for ion gel B it is 7×10^{-3} mS cm^{-1}, in agreement with the higher ionic concentration in ion gel A.

The linear viscoelastic properties of the two ion gels were also studied (Fig. 2b). Ion gel B presents G' values larger than G'' over the entire range of frequencies probed. The slope of G' is $\omega^{0.2}$ confirming the weak frequency dependence. Ion gel B is nearly two orders of magnitude more viscous and one order of magnitude more elastic than ion gel A (at 0.01 rad s^{-1}). This is consistent with the lower content of SMMAS in ion gel A. The storage modulus of ion gel A shows a plateau at low frequencies ($\sim\omega^{0.06}$) and it is higher than its loss counterpart. A crossover point is observed at about 0.64 rad s^{-1}, where G'' overcomes G'. Such a behaviour is unusual for a physical gel wherein G' is always expected to be higher than G''. Therefore, it is more appropriate to name ion gel A *quasi* ion gel A. Despite the high viscosity observed for ion gels, compared to ionic liquid–H_2O mixtures, OECTs with PEDOT:PSS gates show relatively similar values of the modulation.

With the aim to improve the performance of OECTs gated by electrolytes based on Cyphos® IL 106, we used high surface area (1000–2000 m^2 g^{-1}) activated carbon gate electrodes (Fig. ESI 1b (ESI†)).[18,19] Fig. 3 shows transfer curves for pure Cyphos® IL 106 and various Cyphos® IL 106–H_2O mixtures. Transfer curves, where the current is reported on a logarithmic scale, are more appropriate than modulation *vs.* V_g curves, to display the characteristics of devices with high ON/OFF ratios. The OECT ON/OFF ratio strongly depends on the water content in the mixtures and increases from *ca.* 40 (pure Cyphos® IL 106) to *ca.* 5000 (Cyphos® IL 106–H_2O 10% H_2O v/v). Further increasing the H_2O content leads to a decrease of the ON/OFF ratio yielding to a value close to that found for pure Cyphos® IL 106 for 99% H_2O v/v (inset Fig. 3 and Table ESI2 (ESI†)). The transfer curves of the mixture at 99% H_2O v/v and pure Cyphos® IL 106 overlap. For the sake of comparison, transfer characteristics were measured for 0.1 M NaCl and ionic liquid–H_2O mixture at H_2O 70% (v/v): in the latter case higher values of the ON/OFF ratio are observed (Fig. ESI5 (ESI†)). Unlike expected, the highest values of the ON/OFF ratio are not observed in correspondence to the lowest viscosity (Fig. 2a) neither to the highest ionic conductivity. The variation of the ON/OFF ratio with the H_2O content suggests that contributions other than the viscosity and the ionic conductivity of the gating medium have to be considered to completely understand the doping/dedoping process of PEDOT:PSS channels exposed to electrolytes based on Cyphos® IL 106.

Conclusions

In conclusion, we identified two processing approaches to use the highly viscous, hydrophilic, phosphonium-based ionic liquid

Cyphos® IL 106 as the electrolyte in OECTs. The transistor modulation improves from about 0.15 for pure Cyphos® IL 106 to about 0.5 for a binary mixture 5% H_2O v/v. Similar modulations were obtained for an ion gel based on the same ionic liquid, when using PEDOT:PSS gates.

Furthermore, by making use of high surface area activated carbon gates, ON/OFF ratios as high as 5000 were reached in OECTs making use of binary mixtures at 10% H_2O v/v. Experiments with activated carbon gates point to the weak dependence of the OECT performance on ionic conductivity and viscosity of the electrolyte, for values >1 mS cm^{-1} and <500 mPa s, respectively, at least within the time scale of our experiments. Time resolved experiments, at different gate pulse duration, are expected to improve the understanding of the role played by the physicochemical properties of the gating media on the rate of the doping/dedoping process, thus helping to develop high performance OECTs. Our work suggests that the microstructure of the electrolyte (*e.g.* ion association) might also play a role in the doping/dedoping process in OECTs to be applied in bioelectronics.

Experimental

Device fabrication and characterization

An aqueous suspension of poly(3,4-ethylenedioxythiophene):poly(styrenesulfonate), PEDOT:PSS (Clevios™ PH1000, Heraeus Electronic Materials), was mixed with ethylene glycol (EG, Sigma-Aldrich) 25% v/v and with a 0.5% v/v of the surfactant dodecyl benzene sulfonic acid (DBSA, Sigma Aldrich), in order to enhance film electrical conductivity and improve film processability.[35,36] Transistor gate electrodes (only in case of using PEDOT:PSS gate electrode) and channels with a width (W) of 2 mm and a length (L) of 8 mm were patterned on glass slides using a technique described elsewhere.[37] The Clevios™ PH1000/EG/DBSA mixture was spun onto the substrate at 500 RPM for 9 s followed by 1500 RPM for 40 s. The films were then dried on a hot plate at 140 °C for 60 min. The resulting film thickness was about 200 nm. A glass cloning cylinder (VWR), attached to the glass slide with polydimethylsiloxane (Dow Corning Sylgard 184), was used to confine the electrolyte solution upon the channel and the gate electrode of the transistor, the channel being defined by the overlapping of the electrolyte with the organic polymer.

OECT electrical characterization was performed using an Agilent B2902A two-channel source/measure unit, controlled by a LabView software. The gate pulse duration ranged between 50–200 s.

The activated carbon gate electrodes were prepared using carbon paper (Spectracorp 2050, 10 mils) coated with an ink of activated carbon (PICACHEM BP9, 28 mg mL^{-1}) and Nafion (R) binder (2.4 mg mL^{-1}) in isopropanol solvent. Drop casting of the carbon ink was followed by thermal treatment at 60 °C for 24 h to remove the solvent.[19] We used carbon paper stripes 1 cm × 0.4 cm sized.

Electrolyte preparation and characterization

Cyphos® IL 106 (CAS No.: 344774-05-6, product status: developmental), donated by Cytec Industries Inc. (Canada), was mixed with Milli-Q water using a Vortex mixer (VWR). Ion gels based on Cyphos® IL 106 and the triblock copolymer polystyrene-*b*-poly(methyl methacrylate)-*b*-polystyrene (SMMAS, Polymer Source Inc.) were prepared in a nitrogen-purged glove box.[38] Cyphos® IL 106 and SMMAS were co-dissolved in ethyl acetate (EtOAc). SMMAS : Cyphos® IL 106 : EtOAc mass ratios of 1 : 10 : 10 (ion gel A) and 1 : 5 : 10 (ion gel B) were used. The mixture was stirred for 2 h at room temperature.

For OECT fabrication and characterization, 100 μL ion gel precursor were transferred into the glass tube well, which was fixed on an OECT to confine the electrolyte. The device was then cured at 70 °C for 24 h to evaporate the ethyl acetate solvent.

The ionic conductivity of pure Cyphos® IL 106 and Cyphos® IL 106–H_2O binary mixtures (with H_2O 2%, 5%, 10%, 30%, 50%, 70%, 90% and 99% v/v, respectively) was measured with a Traceable Expanded Range Conductivity Meter at room temperature (22 °C). Electrochemical Impedance Spectroscopy (EIS) was used to validate the conductivity meter measurements and to evaluate the ionic conductivity of the ion gels. EIS was carried out with a two-electrode cell with stainless steel electrode plates (electrode geometric area 0.5 cm^2, electrode spacing 0.15 cm), using a BioLogic VSP300. An ac amplitude of 5 mV was used and data were collected in the range 200 kHz–10 mHz, in open circuit conditions. In order to provide a good contact between the ion gel and the stainless steel plates we proceeded as follows. The baking of the ion gel precursor was carried out at 80 °C for 36 h. Afterwards, the plates were immersed in the precursor before performing a final treatment at 50 °C in a vacuum oven for 12 h. The conductivity of the pure ionic liquid and of the ionic liquid–H_2O binary mixtures was calculated from the high frequency real impedance (R), which in turn was evaluated by fitting the EIS Nyquist plots (lines parallel to the imaginary axis) to an RQ equivalent circuit in the high frequency region. For the ion gels, the Nyquist spectrum consisted in a semicircle in the high frequency range, followed by a low frequency tail. In this case, the electrolyte resistance was obtained by fitting the plots to the $(RQ)Q$ equivalent circuit and taking the semicircle diameter as the bulk electrolyte resistance. Q are constant phase elements that model the geometric and double-layer capacitance of the cell.

Rheological measurements on the pure ionic liquid and on the ionic liquid–H_2O binary mixtures were performed at 25 °C using a Physica MCR502 (Anton Paar) rheometer equipped with a rough profiled Couette flow geometry in order to improve the signal. The diameters of the cup and the shaft were 18.09 mm and 16.66 mm, respectively. Shear viscosity data were obtained in simple shear flow using shear rate ramps between 0.01 and 100 s^{-1}. The data reported in Fig. 2a were measured at a shear rate of 1 s^{-1}. The behavior of the different mixtures was essentially Newtonian. Dynamic shear tests were also performed in the linear viscoelastic regime for the pure Cyphos® IL 106 and the Cyphos® IL 106–H_2O mixture at 5% v/v.

For the rheological measurements of the ion gels, a parallel-disk geometry was used. The diameter of the top disk was 2.5 cm. A disposable metal cup (diameter 5.3 cm, depth 0.8 cm) was used as the bottom disk. The ion gel was baked directly on the bottom disk to ensure good adhesion during the rheological

characterization, after confinement into a PDMS well (diameter 2.8 cm, height 0.45 cm). To favor the removal of the ethyl acetate, the solution of the precursors was poured in four steps (one every two hours), while the temperature was kept at 70 °C. Afterwards, the material was left to bake at 50 °C for 48 hours and finally at 70 °C, in a vacuum oven, for 12 hours. The rheological measurements were performed only once per ion gel, and, as a consequence, they only provide the order of magnitude of the measured values.

Acknowledgements

This work is supported by NSERC Discovery grants (F.C. and C.S.) and startup funds from Polytechnique Montréal (F.C.). Z.Y. is grateful to NSERC for financial support through a Vanier Canada Graduate Scholarship and to the Schlumberger Foundation through the Faculty for the Future Fellowship program. F.S. acknowledges financial support by Università di Bologna (Researcher Mobility Program, Italian-Canadian cooperation agreement). We are grateful to Cytec Canada for the donation of the ionic liquid. This work is supported by CMC Microsystems through the programs MNT financial assistance and CMC Solutions.

Notes and references

1 I. S. Martinez and S. Baldelli, in *Ionic Liquids: From Knowledge to Application*, ed. N. V. Plechkova, R. D. Rogers and K. R. Seddon, ACS Symposium Series, 2009, vol. 1030.
2 M. Armand, F. Endres, D. R. MacFarlane, H. Ohno and B. Scrosati, *Nat. Mater.*, 2009, **8**, 621–629.
3 D. R. MacFarlane, J. M. Pringle, P. C. Howlett and M. Forsyth, *Phys. Chem. Chem. Phys.*, 2010, **12**, 1659–1669.
4 M. Galiński, A. Lewandowski and I. Stępniak, *Electrochim. Acta*, 2006, **51**, 5567–5580.
5 T. L. Greaves and C. J. Drummond, *Chem. Rev.*, 2008, **108**, 206–237.
6 Y. Zhu and F. Chen, *Chem. Rev.*, 2014, **114**, 6462–6555.
7 V. I. Pârvulescu and C. Hardacre, *Chem. Rev.*, 2007, **107**, 2615–2665.
8 F. van Rantwijk and R. A. Sheldon, *Chem. Rev.*, 2007, **107**, 2757–2785.
9 S. Y. Yang, F. Cicoira, R. Byrne, F. Benito-Lopez, D. Diamond, R. M. Owens and G. G. Malliaras, *Chem. Commun.*, 2010, **46**, 7972–7974.
10 M. Moniruzzaman, K. Nakashima, N. Kamiya and M. Goto, *Biochem. Eng. J.*, 2010, **48**, 295–314.
11 K. J. Fraser and D. R. MacFarlane, *Aust. J. Chem.*, 2009, **62**, 309–321.
12 K. J. Fraser, E. I. Izgorodina, M. Forsyth, J. L. Scott and D. R. MacFarlane, *Chem. Commun.*, 2007, 3817–3819.
13 Y. Kohno and H. Ohno, *Chem. Commun.*, 2012, **48**, 7119–7130.
14 G. Tarabella, F. M. Mohammadi, N. Coppedè, F. Barbero, S. Iannotta, C. Santato and F. Cicoira, *Chem. Sci.*, 2013, **4**, 1395–1409.
15 T. Fujimoto and K. Awaga, *Phys. Chem. Chem. Phys.*, 2013, **15**, 8983–9006.
16 S. H. Kim, K. Hong, W. Xie, K. H. Lee, S. Zhang, T. P. Lodge and C. D. Frisbie, *Adv. Mater.*, 2013, **25**, 1822–1846.
17 K. H. Lee, S. Zhang, T. P. Lodge and C. D. Frisbie, *J. Phys. Chem. B*, 2011, **115**, 3315–3321.
18 J. Sayago, F. Soavi, Y. Sivalingam, F. Cicoira and C. Santato, *J. Mater. Chem. C*, 2014, **2**, 5690–5694.
19 H. Tang, P. Kumar, S. Zhang, Z. Yi, G. De Crescenzo, C. Santato, F. Soavi and F. Cicoira, *ACS Appl. Mater. Interfaces*, 2015, **7**, 969–973.
20 R. M. Owens and G. G. Malliaras, *MRS Bull.*, 2010, **35**, 449–456.
21 K. Svennersten, K. C. Larsson, M. Berggren and A. Richter-Dahlfors, *Biochim. Biophys. Acta*, 2011, **1810**, 276–285.
22 P. Lin and F. Yan, *Adv. Mater.*, 2012, **24**, 34–51.
23 M. Asplund, T. Nyberg and O. Inganäs, *Polym. Chem.*, 2010, **1**, 1374–1391.
24 W. Liu and J. Holladay, *Catal. Today*, 2013, **200**, 106–116.
25 L. J. A. Conceiçao, E. Bogel-Łukasikb and R. Bogel-Łukasik, *RSC Adv.*, 2012, **2**, 1846–1855.
26 V. Armel, J. Rivnay, G. Malliaras and B. Winther-Jensen, *J. Am. Chem. Soc.*, 2013, **135**, 11309–11313.
27 N. V. Pogodina, M. Nowak, J. Läuger, C. O. Klein, M. Wilhelm and Ch. Friedrich, *J. Rheol.*, 2011, **55**, 241–256.
28 B. Yoo, W. Afzal and M. Prausnitz, *Z. Phys. Chem.*, 2013, **227**, 157–165.
29 J. Jacquemin, P. Husson, A. A. H. Padua and V. Majer, *Green Chem.*, 2006, **8**, 172–180.
30 S. Fendt, S. Padmanabhan, H. W. Blanch and J. M. Prausnitz, *J. Chem. Eng. Data*, 2011, **56**, 31–34.
31 V. Ruiz, T. Huynh, S. R. Sivakkumar and A. G. Pandolfo, *RSC Adv.*, 2012, **2**, 5591–5598.
32 J. Sayago, X. Meng, E. Bourbeau, F. Quenneville, F. Cicoira, F. Soavi and C. Santato, *J. Appl. Phys.*, 2015, **117**, 112809.
33 P. Leleux, C. Johnson, X. Strakosas, J. Rivnay, T. Hervé, R. M. Owens and G. G. Malliaras, *Adv. Healthcare Mater.*, 2014, **3**, 1377–1380.
34 S. P. White, K. D. Dorfman and C. D. Frisbie, *Anal. Chem.*, 2015, **87**, 1861–1866.
35 J. Ouyang, Q. Xu, C.-W. Chu, Y. Yang, G. Li and J. Shinar, *Polymer*, 2004, **45**, 8443–8450.
36 X. Crispin, S. Marciniak, W. Osikowicz, G. Zotti, A. W. D. van der Gon, F. Louwet, M. Fahlman, L. Groenendaal, F. De Schryver and W. R. Salaneck, *J. Polym. Sci., Part B: Polym. Phys.*, 2003, **41**, 2561–2583.
37 F. Cicoira, M. Sessolo, O. Yaghmazadeh, J. A. DeFranco, S. Y. Yang and G. G. Malliaras, *Adv. Mater.*, 2010, **22**, 1012–1016.
38 K. H. Lee, S. Zhang, T. P. Lodge and C. D. Frisbie, *J. Phys. Chem. B*, 2011, **115**, 3315–3321.